Validation of an Analytical Model for the Lift on inline Oscillating Cylinder under Subharmonic Resonance Condition

Krishna Prasad J. S. V. R[1], Shaikh Jaweed S. G.[2], Ansari Khalid A. H.[3]
[1]*Department of Mathematics,* [2]*Department of Humanities and Sciences,* [3] *Department of Mechanical Engineering*
M. J. College, Jalgaon-425001, Maharashtra[1]*, M. H. Saboo Siddik College of Engineering, Byculla, Mumbai*[2]*,*
V. J. T. I College of Engineering, Mumbai, India[3]*.*

Abstract **-** An analytical model for the lift on inline oscillating circular cylinder under subharmonic resonance condition is presented for the validation in the lock-on regime. From numerical simulations, the lift coefficient data of the flow field are obtained over an inline oscillating circular cylinder. The non-linear coupling between the vortex shedding frequency and its third harmonic is characterized by applying spectral analysis to the data. It is concluded from this analysis that the parametrically excited Von der Pol equation should be used to model the lift coefficient on inline oscillating circular cylinder under subharmonic resonance condition. To significantly affect the wake pattern and associated forces, different forcing conditions have been shown on the cylinder.

Keywords **-** Inline oscillations, circular cylinder, Lift model, auto trispectra, subharmonic condition.

I. INTRODUCTION

On circular cylinders drag and lift forces are directly related to the vortex shedding pattern in their wakes. The area of interest would be in reducing these forces, reducing vortex induced-vibrations or augmenting the lift component. Different forcing conditions, to affect the wake pattern and associated forces on the circular cylinder, have been shown significantly and one such condition is oscillation forcing. A significant drag reduction under specific forcing conditions was shown by Tokumaru and Dimostakis [1991], Lu and Sato [1996] and Chou [1997] on rotationally oscillating cylinder. Results of Choi et al. [2002] showed that the maximum amplitude of the lift coefficient is increased in the lock-on region.

The optimal approach to assess effects of cylinder forcing on the wake structure and the lift and drag forces would be a time-domain numerical simulation of the fluid flow and the structure's motion. On the other hand, and for different purposes such as optimization of the forcing parameters, analytical models have been proposed as a more efficient alternative for determining fluctuating forces on oscillating circular cylinder. One of the first models proposed for vortex-induced vibrations of circular cylinder is the one by Hartlen and Currie [1970]. In that model, the lift presented by Rayleigh equation, is linearly coupled to the cylinder's motion. Using a combination of approximate solutions of the Rayleigh and Van der Pol equations and amplitude and phase measurements of higher-order spectral moments, Nayfeh, Owis and Hajj [2003] showed that the lift coefficient,, on the stationary circular cylinders should be modeled by the self-excited Van der Pol equation. Isam and Hajj [2008] also proved the same result for the lift coefficient, $C_L(t)$, on rotationally oscillating cylinder. Gohel et al. [2014] proved that for rotational oscillation Drag and Lift co-efficient is maximum at lock-in $(F = 1)$condition and after increasing or decreasing forcing frequency, the drag and lift co-efficient decreases. For transverse oscillation Drag and Lift co-efficient is increasing as increasing the forcing frequency. The extension of such models to develop an analytical model for the lift force on oscillating circular cylinder would be very beneficial for modeling vortex-induced vibrations, drag reduction or lift augmentation.

In this model we have determined an analytical model for the prediction of the lift on inline oscillating circular cylinder under subharmonic resonance condition. Numerical simulations are performed to generate a data base from which parameters for the developed model are determined. Amplitude and phase measurements from higher order spectral parameters are matched with approximate solutions of the model to characterize the nonlinearities in the model and determine these parameters. Numerical simulations are performed in Ansys Fluent software whereas Fast Fourier Transform (FFT) for the lift time series is performed in Matlab software. Validation of the analytical and numerically obtained lift time series is performed in Microsoft Excel.

II. NUMERICAL SIMULATIONS

Direct Numerical simulations of the unsteady incompressible Navier-Stokes equations for different cases of the flow over an inline oscillating circular cylinder were performed. All simulations were performed at $R_e = {U_\infty D}/{\nu} = 100$. The computational domain was extended 15 cylinder diameters upstream, 15 diameters cross-stream on each side and 40 diameters down-stream. The domain was staggered by

multiple blocks with a quadratic cell type mesh at the boundaries of the domain and triangular cell type mesh near the cylinder wall, in order to provide more faces and to enhance the cell communication and computational accuracy. The minimum and maximum face areas of the cell are 2.099284e-02 $m^2$and 6.568327e-01m^2while minimum Orthogonal Quality is 6.42237e-01and maximum Aspect Ratio is 6.10345e+00. Imposed cylinder oscillations were determined by two parameters, namely, the non-dimensional amplitude, $\dot{\theta}_{max}D/2U_\infty = 0.064$, where $\dot{\theta}_{max}$ is the forcing angular velocity, and the forcing frequency $U_\infty = 0.35$, where f_f is the dimensional forcing frequency. Meshing used is shown in Fig. 1.

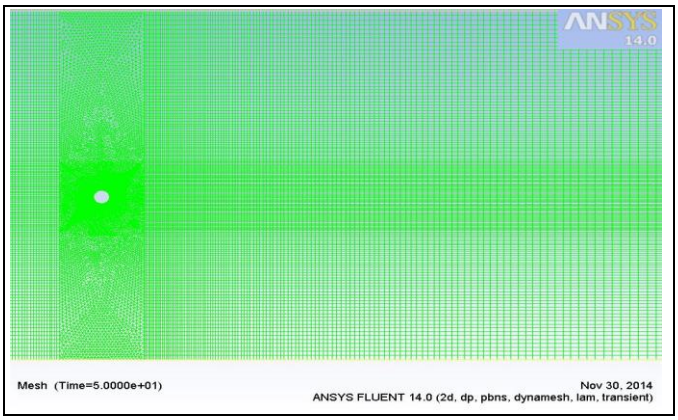

Figure 1: Mesh modeling used for the analysis of lift coefficient over the cylinder under different excitation conditions with minimum and maximum face areas of the cell 2.099284e-02 m^2 and 6.568327e-01 m^2 . The computational domain extended 15 cylinder diameters upstream, 15 diameters cross-stream on each side and 40 diameters down-stream.

III. HIGHER-ORDER SPECTRAL MOMENTS

Traditional signal processing techniques used in data analysis are based on second-order statistics, such as the power spectra which are the Fourier transforms of the second-order correlation functions. These quantities yield an estimate of energy content of the different frequency components in a signal or the coherence between equal frequency components in two signals. In many cases, higher-order spectral moments can be used to obtain more information from signals or time series. In nonlinear systems, frequency components interact to pass energy to other components at their sum and/or difference frequency. Because of this interaction, the phases of the interacting components are coupled. This phase coupling can be used for the detection of nonlinear interactions between frequency components in one or more time series. Faced with an unknown system in terms of its nonlinear characteristic, these moments can be applied to identify quadratic and cubic nonlinearities. The bi-spectrum (by Kim and Powers [1979], Hajj, Miksad and Powers 1997]) which is the next higher order spectrum to power spectrum, has been established as a tool to quantify the level of phase coupling among three frequency components and thus identify quadratic nonlinearities. To this work our particular interest is the tri-spectrum [12], which is the next higher order moment to the bi-spectrum, and which is used to detect and characterize cubic nonlinearities expected to be a part of the lift coefficient.

Above induced higher order spectral moments are multi-dimensional Fourier Transforms of higher-order statistical moments. For any real random process $x(t)$ and its stationary moments up to order n, one could define the n^{th} order moment function as

$$m_n(\tau_1, \tau_2 \dots\dots \tau_{n-1}) = E\{x(t)x(t+\tau_1)\dots\dots x(t+\tau_{n-1})\} \quad (1)$$

Where $E\{\}$ represents ensemble averaging and $\tau_1, \tau_2 \dots\dots \tau_{n-1}$ represents time differences. One can write the following Fourier Transforms pairs for moments as

$$m_2(\tau) \overset{2}{\leftrightarrow} S_{xx}(f) \quad (2)$$

$$m_3(\tau_1, \tau_2) \overset{3}{\leftrightarrow} S_{xxx}(f_1, f_2) \quad (3)$$

$$m_4(\tau_1, \tau_2, \tau_3) \overset{4}{\leftrightarrow} S_{xxxx}(f_1, f_2, f_3) \quad (4)$$

The symbols $\overset{2}{\leftrightarrow}$, $\overset{3}{\leftrightarrow}$ and $\overset{4}{\leftrightarrow}$ denote one-, two- and three-dimensional Fourier Transforms. By Fourier Transforming the second, third and fourth-order moment functions, one obtains, respectively, the auto-power spectrum, auto-bispectrum and auto-trispectrum [12]. Then the hierarchy of higher-order moment spectra is expressed as

$$S_{xx}(f) = \lim_{T \to \infty} \frac{1}{T} E[X_T^*(f) X_T(f)] \quad (5)$$

$$S_{xxx}(f_1, f_2) = \lim_{T \to \infty} \frac{1}{T} E[X_T^*(f_1) X_T^*(f_2) X_T(f_1 + f_2)] \quad (6)$$

$$S_{xxxx}(f_1, f_2, f_3) = \lim_{T \to \infty} \frac{1}{T} E[X_T^*(f_1) X_T^*(f_2) X_T^*(f_3) X_T(f_1 + f_2 + f_3)] \quad (7)$$

Where $X_T(f)$ is the Fourier Transform of $x(t)$ define over a time duration T, and the superscript $*$ is used to denote complex conjugate . The higher-order spectral moments and their normalized counterparts are capable of identifying nonlinear coupling among frequency components and quantifying their phase relations [9, 10, 11]. In this work, we will stress the use of the auto-trispectrum to determine the phase relation between the vortex shedding component and its third harmonic. This relation will be used in determining the parameters of the proposed analytical model.

IV. ANALYTICAL MODEL FOR THE LIFT

The lift coefficient on inline oscillating cylinder is modeled by a parametrically excited van der Pol oscillator which is written as

$$\ddot{C}_L + \omega_s^2 C_L^2 - \mu_v \dot{C}_L + \alpha_v C_L^2 \dot{C}_L + \xi cos(\Omega t + \tau) C_L = 0 \quad (8)$$

Where ω_s is the shedding frequency, μ_v and α_v represents the linear and nonlinear damping coefficients, ξ and τ are respectively the amplitude and phase of the external harmonic Function which represents the inline oscillations.

To balance the damping, nonlinearities and parametric excitation in equation (8), μ_v, $\alpha_v$and ξ are scaled as $\epsilon\mu_v$, $\epsilon\alpha_v$and $\epsilon\xi$. The parametrically excited van der Pol equation is then written as

$$\ddot{C}_L + \omega_s^2 C_L^2 - \epsilon\mu_v \dot{C}_L + \epsilon\alpha_v C_L^2 \dot{C}_L + \epsilon\xi cos(\Omega t + \tau) C_L = 0 \quad (9)$$

Using the method of multiple scales [13, 14], an analytical approximate solution is derived for Equation (9) for the subharmonic resonance condition set by

$$\Omega = 2\omega_s + \epsilon\sigma \quad (10)$$

Where σ is the detuning parameter. The approximate solution, under this condition, is of the form

$$C_L(t) \approx acos\left(\frac{\Omega}{2}t + \frac{\tau}{2} - \frac{\gamma}{2}\right) + \frac{a^3\alpha_v}{32\omega_s} cos\left(3\left(\frac{\Omega}{2}t + \frac{\tau}{2} - \frac{\gamma}{2}\right) + \frac{\pi}{2}\right) + \frac{a\xi}{16\omega_s^2}\cos\left(\frac{3\Omega}{2}t + \frac{3\tau}{2} - \frac{\gamma}{2}\right) + \frac{a^3\alpha_v\xi}{256\omega_s^3}\cos\left(\frac{5\Omega}{2}t + \frac{5\tau}{2} - \frac{3\gamma}{2} + \frac{\pi}{2}\right) + \frac{a\xi^2}{768\omega_s^4}\cos\left(\frac{5\Omega}{2}t + \frac{5\tau}{2} - \frac{\gamma}{2}\right) \quad (11)$$

Where γ is given by

$$\gamma = \epsilon\sigma t - \tau - 2\beta \quad (12)$$

In equation (11), the amplitude a and phase γ are governed by

$$\dot{a} = \frac{\mu_v}{2}a - \frac{\alpha_v}{8}a^3 - \frac{a\xi}{4\omega_s} sin\gamma \quad (13)$$

$$\dot{\gamma} = \sigma - \frac{\xi}{2\omega_s} cos\gamma \quad (14)$$

An examination for the expression of γ reveals its dependency on the phase of parametric excitation, τ and the phase of the response, β. For steady-state oscillations, i.e., when a and γ are constants in equations (13) and (14), the solution given in equation (11) represents a periodic motion which can be written in complex form as

$$C_L(t) \approx \frac{a}{2}\left\{e^{i\left(\frac{\Omega}{2}t+\frac{\tau}{2}-\frac{\gamma}{2}\right)} + e^{-i\left(\frac{\Omega}{2}t+\frac{\tau}{2}-\frac{\gamma}{2}\right)}\right\} + \frac{a^3\alpha_v}{64\omega_s}\left\{e^{3i\left(\frac{\Omega}{2}t+\frac{\tau}{2}-\frac{\gamma}{2}\right)+i\frac{\pi}{2}} + e^{-3i\left(\frac{\Omega}{2}t+\frac{\tau}{2}-\frac{\gamma}{2}\right)-i\frac{\pi}{2}}\right\} + \frac{a\xi}{32\omega_s^2}\left\{e^{i\left(\frac{3\Omega}{2}t+\frac{3\tau}{2}-\frac{\gamma}{2}\right)} + e^{-i\left(\frac{3\Omega}{2}t+\frac{3\tau}{2}-\frac{\gamma}{2}\right)}\right\} + \frac{a^3\alpha_v\xi}{512\omega_s^3}\left\{e^{i\left(\frac{5\Omega}{2}t+\frac{5\tau}{2}-\frac{3\gamma}{2}+\frac{\pi}{2}\right)} + e^{-i\left(\frac{5\Omega}{2}t+\frac{5\tau}{2}-\frac{3\gamma}{2}+\frac{\pi}{2}\right)}\right\} + \frac{a\xi^2}{1536\omega_s^4}\left\{e^{i\left(\frac{5\Omega}{2}t+\frac{5\tau}{2}-\frac{\gamma}{2}\right)} + e^{-i\left(\frac{5\Omega}{2}t+\frac{5\tau}{2}-\frac{\gamma}{2}\right)}\right\} \quad (15)$$

The Fourier transform of $C_L(t)$, represented by $L(\omega)$, is then given by -

$$L(\omega) \approx \frac{a}{2}\left\{e^{i\left(\frac{\tau}{2}-\frac{\gamma}{2}\right)}\delta\left(\omega - \frac{\Omega}{2}\right) + e^{-i\left(\frac{\tau}{2}-\frac{\gamma}{2}\right)}\delta\left(\omega + \frac{\Omega}{2}\right)\right\} + \frac{a^3\alpha_v}{64\omega_s}\left\{e^{3i\left(\frac{\tau}{2}-\frac{\gamma}{2}\right)+i\frac{\pi}{2}}\delta\left(\omega - \frac{3\Omega}{2}\right) + e^{-3i\left(\frac{\tau}{2}-\frac{\gamma}{2}\right)+i\frac{\pi}{2}}\delta\left(\omega + \frac{3\Omega}{2}\right)\right\} + \frac{a\xi}{32\omega_s^2}\left\{e^{i\left(\frac{3\tau}{2}-\frac{\gamma}{2}\right)}\delta\left(\omega - \frac{3\Omega}{2}\right) + e^{-i\left(\frac{3\tau}{2}-\frac{\gamma}{2}\right)}\delta\left(\omega + \frac{3\Omega}{2}\right)\right\} + \frac{a^3\alpha_v\xi}{512\omega_s^3}\left\{e^{i\left(\frac{5\tau}{2}-\frac{3\gamma}{2}+\frac{\pi}{2}\right)}\delta\left(\omega - \frac{5\Omega}{2}\right) + e^{-i\left(\frac{5\tau}{2}-\frac{3\gamma}{2}+\frac{\pi}{2}\right)}\delta\left(\omega + \frac{5\Omega}{2}\right)\right\} + \frac{a\xi^2}{1536\omega_s^4}\left\{e^{i\left(\frac{5\tau}{2}-\frac{\gamma}{2}\right)}\delta\left(\omega - \frac{5\Omega}{2}\right) + e^{-i\left(\frac{5\tau}{2}-\frac{\gamma}{2}\right)}\delta\left(\omega + \frac{5\Omega}{2}\right)\right\} \quad (16)$$

On examining the expression for $L(\omega)$, it is noted that the solution contains components with frequencies at $\frac{\Omega}{2}$, $\frac{3\Omega}{2}$, $\frac{5\Omega}{2}$. In terms of their amplitudes and phases, these components are written as

$$L\left(\frac{\Omega}{2}\right) = \frac{a}{2}e^{i\left(\frac{\tau}{2}-\frac{\gamma}{2}\right)} \quad (17)$$

$$L\left(\frac{3\Omega}{2}\right) = \frac{a^3\alpha_v}{64\omega_s}e^{3i\left(\frac{\tau}{2}-\frac{\gamma}{2}\right)+i\frac{\pi}{2}} + \frac{a\xi}{32\omega_s^2} \quad (18)$$

$$L\left(\frac{5\Omega}{2}\right) = \frac{a^3\alpha_v\xi}{512\omega_s^2}e^{i\left(\frac{5\tau}{2}-\frac{3\gamma}{2}\right)+i\frac{\pi}{2}} + \frac{a\xi^2}{1536\omega_s^4}e^{i\left(\frac{5\tau}{2}-\frac{\gamma}{2}\right)} \quad (19)$$

The auto-trispectrum defined in equation (7) and given by

$$S_{lll}(\omega_k, \omega_l, \omega_m) = \lim_{T \to \infty}\frac{1}{T}E[L^*(\omega_k)L^*(\omega_l)L^*(\omega_m)L(\omega_k + \omega_l + \omega_m)] \quad (20)$$

gives the following expression for $\left(\omega_k = \omega_l = \omega_m = \frac{\Omega}{2}\right)$

$$S_{lll}\left(\frac{\Omega}{2}, \frac{\Omega}{2}, \frac{\Omega}{2}\right) \approx \frac{a^6\alpha_v}{512\omega_s}e^{i\frac{\pi}{2}} + \frac{a^4\xi}{256\omega_s^2} \quad (21)$$

The magnitude and phase of the auto-trispectrum $S_{lll}\left(\frac{\Omega}{2}, \frac{\Omega}{2}, \frac{\Omega}{2}\right)$ depend on the coefficient of the cubic nonlinearity α_v and the parametric excitation coefficient ξ. The real and imaginary parts of auto- trispectrum $S_{lll}\left(\frac{\Omega}{2}, \frac{\Omega}{2}, \frac{\Omega}{2}\right)$, can be used to identify the parametric excitation coefficient ξ and the coefficient of the cubic nonlinearity α_v.

The normalized auto-trispectrum, namely, the auto-tricoherence for $\left(\omega_k = \omega_l = \omega_m = \frac{\Omega}{2}\right)$ is written as

$$t^2\left(\frac{\Omega}{2}, \frac{\Omega}{2}, \frac{\Omega}{2}\right) \approx \frac{\left|S_{lll}\left(\frac{\Omega}{2'}\frac{\Omega}{2'}\frac{\Omega}{2}\right)\right|^2}{\left|L\left(\frac{\Omega}{2}\right)L\left(\frac{\Omega}{2}\right)L\left(\frac{\Omega}{2}\right)\right|^2\left|L\left(\frac{3\Omega}{2}\right)\right|^2} \quad (22)$$

A unit value of the auto-tricoherence indicates perfect cubic phase coupling, a zero value indicates no coupling and any value in between indicates partial coupling. The auto-tricoherence is a necessary quantity that should be used to determine the extent of coupling in a time series and the validity of using the magnitude and phase of the trispectrum to model physical phenomenon by the Van der Pol equation.

For the parametrically excited van der Pol equation with the case of subharmonic resonance $(\Omega \approx 2\omega_s)$, the steady-state value of the amplitude a and phase γ can be obtained by setting $\dot{a} = 0$ and $\dot{\gamma} = 0$ in equations (13) and (14). That is

$$0 = \frac{\mu_v}{2}a - \frac{\alpha_v}{8}a^3 - \frac{a\xi}{4\omega_s}sin\gamma \quad (23)$$

$$0 = \sigma - \frac{\xi}{2\omega_s}cos\gamma \quad (24)$$

To determine the damping and nonlinear coefficients, as well as the excitation coefficient in the parametrically excited van der Pol equation, we represent the lift coefficient as

$$C_L(t) \approx a_1 cos\left(\frac{\Omega}{2}t + \beta_1\right) + a_3 cos\left(\frac{3\Omega}{2}t + \beta_3\right) + a_5 cos\left(\frac{5\Omega}{2}t + \beta_5\right) \quad (25)$$

On comparing equation (25) with equation (11), and using equations (13), (14) and (21), one obtains

$$\alpha_v = \frac{512\omega_s Im\left|S_{lll}\left(\frac{\Omega}{2},\frac{\Omega}{2},\frac{\Omega}{2}\right)\right|}{a_1^6} \quad (26)$$

$$\xi = \frac{256\omega_s^2 Re\left[S_{lll}\left(\frac{\Omega}{2},\frac{\Omega}{2},\frac{\Omega}{2}\right)\right]}{a_1^4} \quad (27)$$

$$cos\gamma = \sigma\frac{2\omega_s}{\xi} \quad (28)$$

$$\mu_v = \frac{1}{4}\alpha_v a_1^2 + \frac{\xi}{2\omega_s}sin\gamma \quad (29)$$

and

$$\tau = 2\phi\left(L\left(\frac{\Omega}{2}\right)\right) + \gamma \quad (30)$$

Where $\phi\left(L\left(\frac{\Omega}{2}\right)\right)$ is the phase of the frequency component $L\left(\frac{\Omega}{2}\right)$. The set of equations 26 – 30 shows how the different spectral parameters can be used to predict the parameters of the model presented in equation (8).

V. RESULTS AND DISCUSSIONS

Vorticity contour in the wake of the cylinder subjected to inline oscillations under subharmonic resonance condition is presented in Fig. 2. The vortex shedding pattern presented in Fig. 2 is compared with the pattern obtained by Jaweed S. et al. [15] in case of inline oscillating cylinder under no resonance condition as presented in Fig. 3. Vortex shedding patterns observed in both the cases are nearly similar.

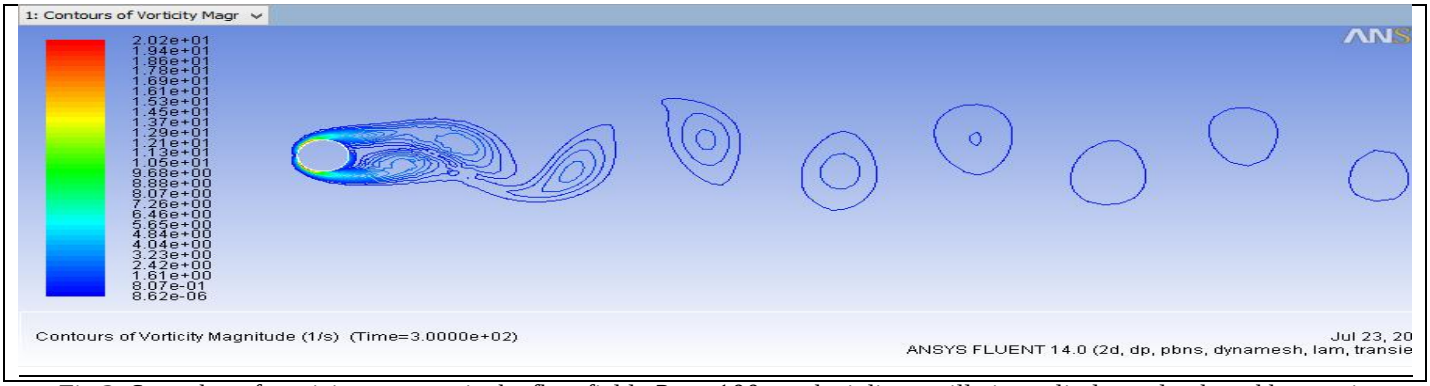

Fig 2: Snap shot of vorticity contours in the flow field, $R_e = 100$, on the inline oscillating cylinder under the subharmonic resonance condition. Forcing condition: $\dot{\theta}_{max}D/2U_\infty = 0.064, f_f D/U_\infty = 0.35$

Fig 3: Snap shot of vorticity contours in the flow field, $R_e = 100$, on the inline oscillating cylinder under no resonance condition. Forcing condition: $\dot{\theta}_{max}D/2U_\infty = 0.064, f_f D/U_\infty = 0.35$, adapted from Jaweed S. et al. [2015]

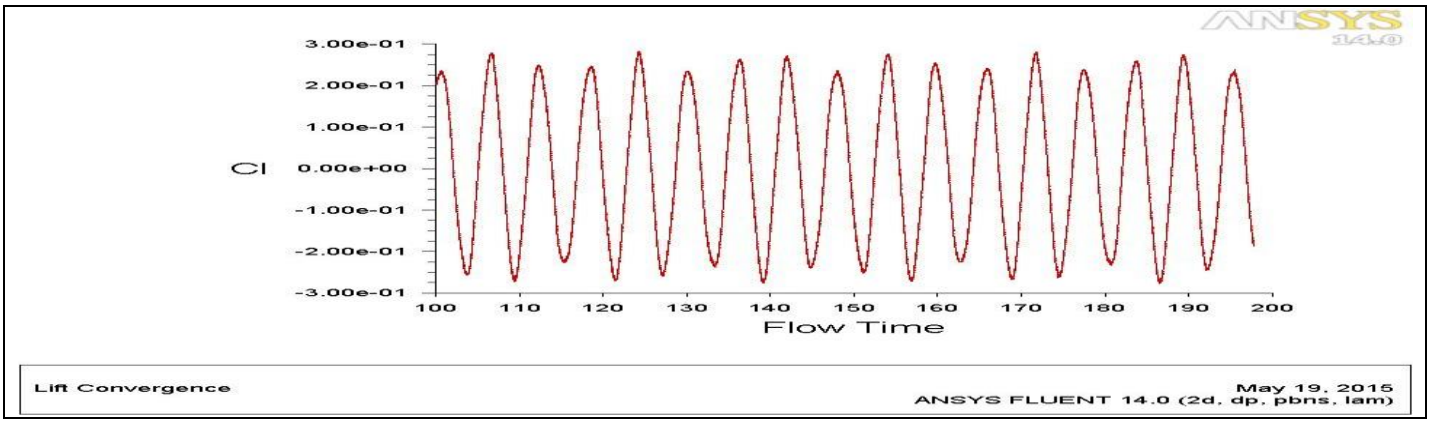

(a)

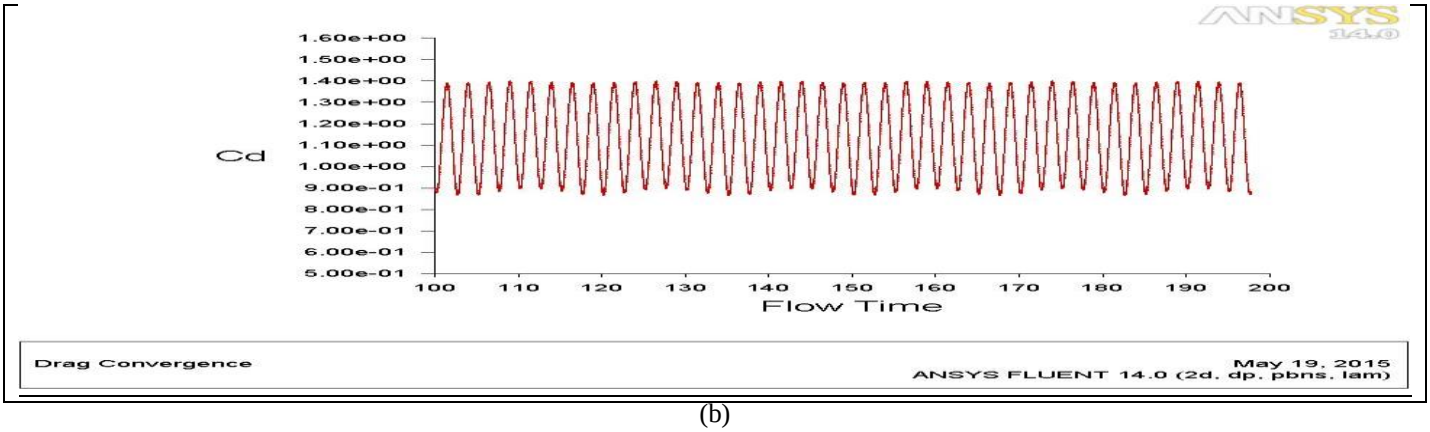

(b)

Fig 4: Time histories of the lift (a) and drag (b) coefficients on the inline oscillating cylinder under subharmonic resonance condition. Forcing condition: $\dot{\theta}_{max}D/2U_\infty = 0.064, f_f D/U_\infty = 0.35$

In case of inline oscillating cylinder under subharmonic resonance condition, the cylinder was forced to oscillate at a frequency $\Omega = 0.35$Hz at a non-dimensional amplitude $^{y}/_{D} = 0.064$. The Reynolds number was set at 100. Spectral analysis was performed on the lift time series that is plotted in Fig. 4.The power spectrum of the resulting lift coefficient, using Matlab, obtained from Ansys Fluent simulations is shown in Fig. 6. The spectrum shows several peaks. In this figure, peaks at $\frac{\Omega}{2}$, $\frac{3\Omega}{2}$ and $\frac{5\Omega}{2}$ are noted. These peaks show that there is a subharmonic resonance. Values of spectral parameters f, a_1, a_3, a_5 and $\phi\left(L\left(\frac{\Omega}{2}\right)\right)$, as obtained from the spectral analysis, are shown in Table 1. These values are then used to estimate ξ, τ , γ, μ_v and α_v based on equations 24-28. These model parameter values are presented in Table 2. Values of the parameters presented in Table 2 were then used to predict the steady-state lift by integrating equation (8). To verify the lift coefficient model, we compare the simulated and modeled time series for lift coefficients. Result of validation is obtained in Microsoft Excel and presented in Fig. 5. A comparison of the lift time series show that the parametric excitation models along with the derived parameters yield the right frequency and amplitude variations. The graph of trispectrum obtained from Matlab is shown in Fig. 7.

Table 1: Lift spectral parameters for the inline oscillating cylinder under sub-harmonic resonance condition-

Ω (Hz)	0.35
$^{y}/_{D}$	0.064
f (Hz)	0.1667
a_1	0.1754
a_3	0.0005652
a_5	0.0002067
$\phi\left(L\left(\frac{\Omega}{2}\right)\right)(rad)$	4.613

Table 2: Lift model parameters in parametrically excited van der Pol equation under subharmonic resonance condition

$\Omega(Hz)$	0.35
y/D	0.064
$f(Hz)$	0.1667
$\xi(fromS_{IIII})$	0.1108
$\tau(rad)$	11.1321
μ_v	0.0379
$\alpha_v(fromS_{IIII})$	-2.1915

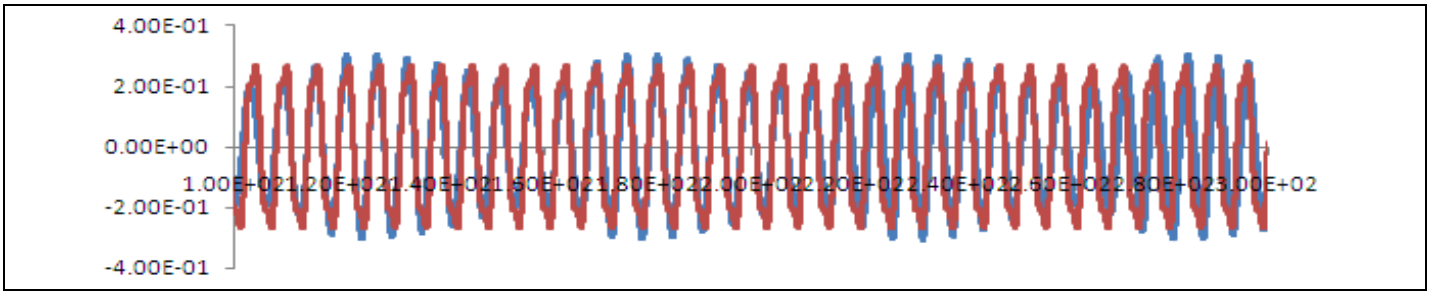

Fig 5: Comparison of the analytically modeled (red line) and numerically simulated (blue line) lift time series on an inline oscillating cylinder under the subharmonic resonance condition. Forcing condition: $\dot{\theta}_{max}D/2U_\infty = 0.064, f_f D/U_\infty = 0.35$

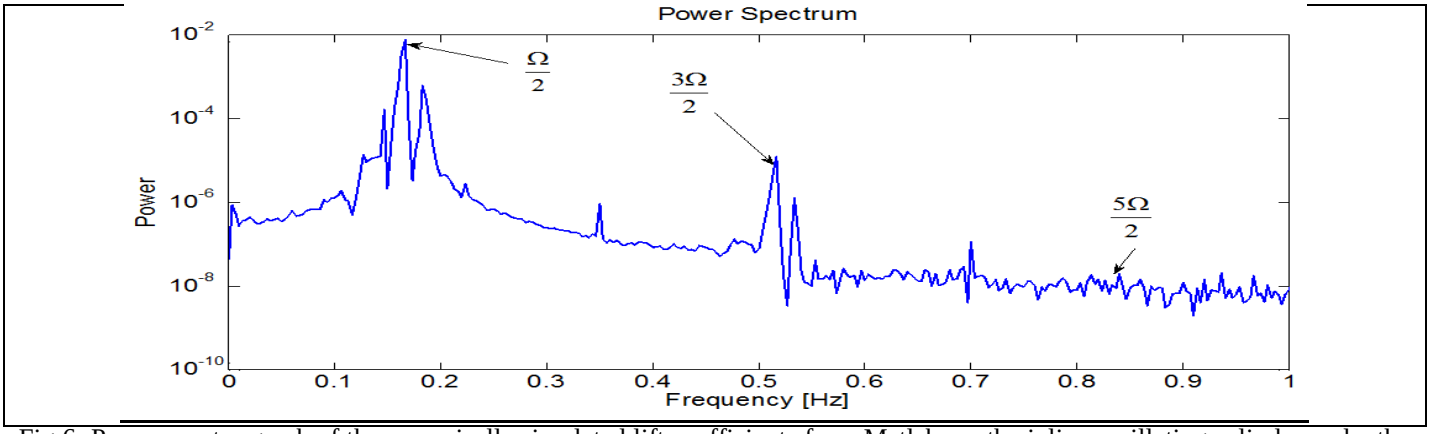

Fig 6: Power spectra graph of the numerically simulated lift coefficients from Matlab, on the inline oscillating cylinder under the subharmonic resonance condition. Forcing condition: $\dot{\theta}_{max}D/2U_\infty = 0.064, f_f D/U_\infty = 0.35$

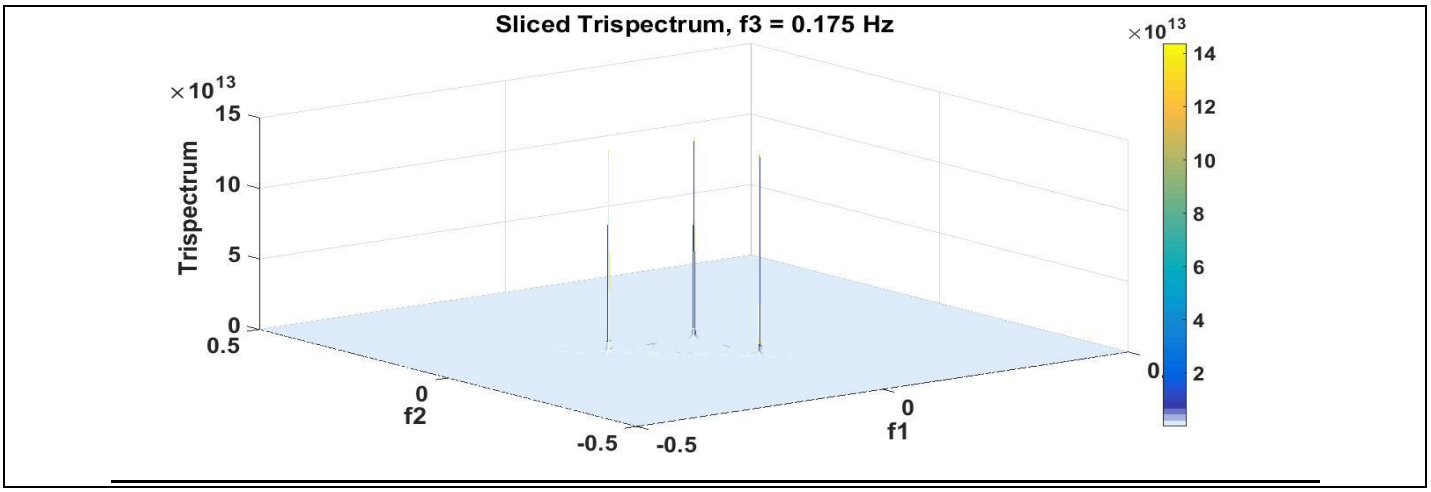

Fig 7: Graph of trispectrum of the numerically simulated lift coefficients from Matlab, on an inline oscillating cylinder under the subharmonic resonance condition. Forcing condition: $\dot{\theta}_{max}D/2U_\infty = 0.064, f_f D/U_\infty = 0$

VI. CONCLUSIONS

In this study, an analytical model for the prediction of the lift on inline oscillating cylinder under subharmonic resonance condition has been developed. The parameters of the developed model were determined from a numerical simulation of the flow field using higher-order spectral analysis of the lift data. Higher-order spectral analysis of the lift data yielded relevant quantities that were matched with approximate solutions of the assumed model. Fast Fourier Transform (FFT) was performed using Matlab. The validity of the model has been demonstrated by comparing time domain characteristics of the analytically modeled lift coefficient with the numerically simulated data. Numerical simulation using Ansys fluent software is performed to validate the analytical model for the lift on an inline oscillating cylinder under subharmonic resonance condition. The perfect matching of the lift time series shows that Van der Pol oscillator should be used to model the lift on inline oscillating cylinder under subharmonic resonance condition.

VII. REFERNCES

[1]. Tokumaru P. T., Dimotakis P. E.: Rotary oscillation control of a cylinder wake. J. Fluid Mech. 224, 77-*90* (1991).

[2]. Lu X.Y., Sato J.: A numerical study of flow past a rotationally oscillating circular cylinder. J. Fluids Struct. 10, 829-849 (1996).

[3]. Chou M. H.: Synchronization of vortex shedding from a cylinder under rotary oscillation. Comput. Fluids. 26, 755-774 (2001).

[4]. Choi S., Choi K., Kang S.: Characteristics of flow over a rotationally oscillating cylinder at low Reynolds number. Phys. of Fluids. 14(8), 2767-2777 (2002).

[5]. Hartlen R. T., Currie I. G.: Lift-Oscillator Model of Vortex-Induced Vibrations. Journal of Engineering Mechanics. 96(5), *577*–591 (1970).

[6]. Nayfeh A. H, Owis F., Hajj M.R.: A model for the coupled lift and drag on a circular cylinder. Proc. of DETC 2003, ASME 19th Biennial Conference on Mechanical Vibrations and Noise, Chicago, IL, USA, DETC2003/VIB-48455 (2003).

[7]. Isam Janajreh, Muhammad Hajj.: An Analytical Model for the Lift on a Rotationally Oscillating Cylinder. BBAA VI International Colloquium on: Bluff Bodies Aerodynamics & Applications, Milano, Italy, July, 20–24 (2008).

[8]. Ankit R. Gohel, Balkrushna A Shah , Absar M Lakdawala.: Numerical Investigation on Flow over Rotational and Transverse Oscillating Circular Cylinder, FMFP 2014 international conference on: Computational Fluid Dynamics, IIT Kanpur, India, December 13 (2014).

[9]. Kim Y.C., Powers E. J.: Digital bispectral analysis and its applications to nonlinear wave interactions. IEEE Trans. Plasma Sci. PS-7, 120-131 (1979).

[10]. Hajj M. R., Miksad R. W., Powers E. J.: Fundamental-subharmonic interaction: effect of the phase relation. Journal of Fluid Mechanics. 256, *403*- 426 (1993).

[11]. Hajj M. R., Miksad R. W., Powers E. J.: Perspective: measurements and analysis of nonlinear wave interactions with higher-order spectral moments. Journal of Fluids Engineering. 119*(1)*, *3*-13, (1997).

[12]. Powers E. J., Im S.: Introduction to higher-order statistical signal processing and its applications. in: Higher-Order Statistical Signal Processing (Boashash, Powers & Zoubir eds.) Longman, Australia (1995).

[13]. Nayfeh A. H. *Perturbation Methods*, Wiley, New York (1973).

[14]. Nayfeh A. H. *Introduction to Perturbation Techniques*, Wiley, New York (1981).

[15]. Jaweed S., Khalid A., Krishna Prasad J. S. V.R.: An Analytical Model for the prediction of Lift on Rotationally Oscillating Cylinder under no resonance condition with soft excitation. International Journal of Application or Innovation in Engineering & Management (IJAIEM). 4(4), 207-214 (2015).